Supporting Information

Bottos et al. 10.1073/pnas.0809510106

SI Text

R1: Neurexin and Neuroligin Expression in Large Blood Vessels. Immunohistochemical analysis revealed that the polyclonal anti-NRXN antibody stained many layers of mural cells in addition to the nerve tissue (Fig. 1*B*) in a cross-section of a multilayered vessel from the chicken brain. These cells were defined as vascular SMCs because they were not stained by the EC marker FVIII (Fig. 1*A*) but were co-stained by an α-SMA antibody (Fig. 1*C*). The same arrangement was visible in 2 arterial vessels of the embryo chicken kidney (E11) in which the pan-neurexin staining (Fig. 1, *E* and *F*) excluded the ECs (Fig. 1*D*) but clearly overlapped with the α-SMA expression (Fig. 1*G*), which extended beyond these layers. The shorter development times of the immunohistochemical reaction revealed that the highest levels of neurexin expression were found within discrete cellular and subcellular patches (Fig. 1, *H*, *L*, and *Q*). In a mouse kidney artery, the polyclonal anti-NRXN antibody signals also excluded the EC lining (Fig. 1 *M*) and produced spot-like staining in the blood vessel media (Fig. 1*N*). Further analysis demonstrated that neuroligin was expressed with high preference in the ECs of multilayered arterial vessels in the adult chicken brain (Fig. 1, *P* and *R*), whereas neurexin was produced by the surrounding SMCs.

R2: Immunohistochemical Analysis of Neurexin and Neuroligin Expression in the Vascular System of the Brain. We analyzed the vasculature of 6 brains from E18 chicken embryos and 6 adult mouse brains.

In the chicken embryo brain, neurexin and neuroligin are expressed ubiquitously with several enriched areas in the pallium, midbrain, and cerebellum that often overlap with the staining of synaptic vesicle protein 2 (SV2) (Fig. S4*A*). The vasculature is clearly visualized by α-SMA detection. The walls of large extra-parenchymatic vessels are strongly marked by the anti-NRXN and anti-NLGN antibodies. The expression of neurexin and neuroligin seems to decrease when the vessels enter the parenchyma, become thinner, and lose their muscular coating. The dense neuronal staining makes it difficult to detect capillaries, but we could provide examples of small vessels stained by the anti-NRXN and anti-NLGN antibodies.

In the mouse brain, neurexin and neuroligin expression is quite diffuse, but the immunohistochemical analysis on sagittal sections shows an enrichment of neurexin, similar to that of synaptophysin, in areas such as the hippocampus, neocortex, and cerebellum (Fig. S5). Neuroligin expression appears much more homogeneous, but enrichment in the cortex and in hippocampal pyramidal neurons (Fig. S5) also is visible. The cerebral vasculature is characterized by strong expression of neuroligin throughout the vessel wall of all large extra-parenchymatic arteries and veins, whereas neurexin staining is weaker and is confined to a subset of α-SMA–positive medial cells. Intraparenchymal vessels that express α-SMA also express both neurexin and neuroligin. As in the chicken brain, capillaries were difficult to detect by neurexin and neuroligin antibodies, but we were able to identify examples of small vessels expressing both proteins. Future studies using isoform-specific antibodies against these proteins combined with confocal microscopy analysis could reveal smaller vessels and capillaries more clearly.

The tables in Figs. S4 and S5 also provide a general quantification of the levels of neurexin and neuroligin expression in cerebral vessels. For the well-structured vessels we also provide a quantification of neurexin and neuroligin espression relative to the expression of ECs and SMCs.

R3: Absence of Nervous Markers in Chicken Arteries. Blood vessels in animals are innervated by the autonomous nervous system (1) or, in the brain, by local GABA interneurons through specific structures called "varicosities" (2). Although, in general, autonomic nerves and varicosities never reach the most luminal region of the chicken arteries, where we detected neurexin and neuroligin expression, it was important to exclude the possibility that we were isolating nerve tissue along with arteries. For this reason, we always stripped off the adventitial layer and made sure that no markers of the nervous system were present. Fig. S6*A* shows that the markers tyrosine hydroxylase, neurofilament, and microtubule-associated protein 2 (MAP2) specifically stained regions of the chicken brain. However, they did not stain randomly chosen sections of stripped blood vessels.

R4: Expression of Neurexin and Neuroligin Isoforms in Chicken Arteries. This set of data is part of the analysis of the expression of neurexin and neuroligin in surgically extracted chicken embryo mesenteric arteries.

The table in Fig. S6*B* shows that α and β forms of neurexin 1 and 3 and neuroligin 1–4 were expressed in chicken embryo arteries. We did not investigate neurexin 2 expression because we could not isolate this gene during our *in silico* analysis of the chicken genome. Interestingly, we isolated a long form of neurexin 3β (deposited as *Gallus gallus* NRXN3β, EU702429) that was not present in the brain (Fig. S6*B*, *Right*).

R5: Chicken Aortic Ring Assay and the Effect of Anti-βNRXN Antibody Treatment. We adapted the aortic ring assay (3) using E18 chicken embryo arteries that were embedded in a pro-angiogenic matrix (Matrigel, a reconstituted basal membrane constituted by ECM proteins and growth factors) for 3 to 4 days and allowed to sprout. The subsequent immunohistochemical analysis of the rings revealed that the original histological structure of the section was considerably altered (Fig. S6*C*, *Middle*). In particular, in these conditions cells expressing neurexin, neuroligin, and α-SMA were no longer found in single continuous layers of cells but were scattered throughout the ring and among sprouted cells within the Matrigel matrix. Of particular interest was the complete overlap between neuroligin- and VEGFR2-expressing cells in the sprouted region (Fig. S6*C*, *Bottom*). Although this assay demonstrated the involvement of neurexin- and neuroligin-expressing cells in vascular remodeling, we have found that the sprouting of these rings is very peculiar. In fact, in this model there is a paucity of EC during the first days of sprouting, and mesenchymal/fibroblastic cells lead the process, giving rise to a very intricate mesh of tubules in which EC sprouts, although significantly present (Fig. S6*C*), lag behind. Overall, this model seems a poor one for studying angiogenesis, because it appears similar to the sprouting of myofibroblast (4). In this system, the anti-βNRXN antibody never significantly influenced the sprouting (Fig. S6*D*). For this reason we chose the CAM assay as a physiological model of angiogenesis.

R6: in Vitro Assays for the Characterization of Anti-βNRXN Antibody Activity in Angiogenesis. Among the plethora of possible explanations for the anti-angiogenic effect of the anti-βNRXN antibody, we considered that this reagent could affect cellular processes related to angiogenesis in cells that express neurexin

in vivo. To address this possibility, we extracted mural cells from chicken embryo aorta (Ao cells); however, as with all other cell types that we tested (see *SI Text, R7*), no appreciable amount of neurexin expression was maintained after in vitro culture. To characterize anti-βNRXN antibody activity, we overcame the low expression level of neurexin 1β in Ao cells through its overexpression mediated by a lentiviral vector (Fig. S8*A*).

We analyzed the role of neurexin 1β overexpression and the effect of anti-βNRXN antibody in several in vitro assays (Fig. S8).

(*i*) Adhesion and migration of Ao cells overexpressing neurexin 1β on laminin or collagen coated plates were not affected. The haptotaxis migration toward laminin was not impaired by neurexin overexpression or anti-βNRXN antibody treatment (Fig. S8*B*). The adhesive properties on laminin and collagen were largely unaffected by the overexpression of neurexin 1β, and the anti-β NRXN antibody did not induce a significant effect (Fig. S8*C*).

(*ii*) The expression of neurexin 1β in Ao cells did not affect proliferation and survival in basal conditions or after FGF-2 stimulation. The treatment with the anti-βNRXN antibody also showed no effect (Fig. S8, *D* and *E*).

Within this set of experiments we also tested the in vitro cell aggregation mediated by neurexin and neuroligin. Pools of PAE cells overexpressing either β neurexin or neuroligin (Fig. S8*F*) were mixed in the presence of calcium ions (an assay modified from procedures given in ref. 5). The anti-βNRXN antibody did not significantly reduce the number of aggregates versus the control antibody (Fig. S8*G*).

R7: Analysis of Neurexin and Neuroligin Expression in Cultured Cells. We performed a set of expression analyses for neurexin and neuroligin in cultured cells including human ECs, fibroblast cells, and VSMCs (Fig. S9). Several neuroligins were easily detected in different cell types. Through immunoprecipitation, we demonstrated the expression of neuroligin in ECs of micro- and macrovascular origin (Fig. S9*A*). Furthermore, we accurately described by RT-PCR which neuroligin isoforms are expressed in ECs and the respective splicing patterns (Fig. S9*B*). On the other hand, none of the tested cells produced appreciable amounts of neurexin. Because the cultured VSMCs that we used derived from mature blood vessels, this observation could be explained by the heterogeneity of the VSMC population in the blood vessel media (6) (as supported by our own neurexin staining, see Fig. 1, *H*, *L*, and *N*) or, more likely, by the "dedifferentiation" process that VSMCs experience during in vitro culture (7, 8).

R8: Modulation of Neurexin and Neuroligin Transcripts in 3D Co-Cultures of ECs and Fibroblasts. To begin the investigation of the possibility that neurexin and neuroligin play a role in cell differentiation during blood vessel development and maturation, we performed the following set of experiments.

Based on the well-known relationships between fibroblasts, VSMCs, and ECs, in terms of ontogeny and paracrine influences (9, 10), we set up an in vitro co-culture system that recapitulates interactions between the EC and the mural cell precursor. ECs and fibroblasts were co-cultured in a 3D environment (spheroids), and the neurexin and neuroligin transcripts were analyzed by qPCR. The results support a role for these proteins in vascular development. Indeed, Fig. S9*C* shows that in the spheroids neurexin and neuroligin and some of their intracellular partners, along with known mediators of vascular maturation (Caldesmon 1, PDFG-β receptor, TGF-β, and angiopoietins), are modulated at the transcript level against the control monolayer co-culture.

Materials and Methods

Cell Lines. Human dermal fibroblast (NHDF) and human umbilical artery SMCs were purchased from Clonetics (Cambrex Bio Science) and cultured according to the manufacturer's instructions.

The primary culture of chicken embryo fibroblasts was extracted from E10 chicken embryos using standard techniques (11), cultured in DMEM (Cambrex Bio Science), 10% FBS (Gibco; Invitrogen), penicillin (500 U/mL), and streptomycin (100 μg/mL), and subcultured until passage number 3.

Human umbilical vein ECs (HUVEC) were cultured with common protocols. Human umbilical artery ECs were extracted from umbilical cord arteries and cultured in EGM-2 medium (Clonetics, Cambrex Bio Science) on gelatin-coated dishes. Human microvascular ECs were cultured as previously described (12).

PAE cells (provided by J. Waltenberger, University Medical Center, Ulm, Germany) were cultured in Ham's F12 medium (Clonetics, Cambrex Bio Science), 10% FBS (Gibco; Invitrogen), penicillin (500 U/mL), and streptomycin (100 μg/mL). PAE clones permanently overexpressing neurexin 1β-GFP or neuroligin 1 were maintained in Geneticin Selective Antibiotic (Gibco; Invitrogen).

The MDA-MB-435 cell line (provided by ATCC- LGC Standards s.r.l.) was cultured in DMEM (Clonetics; Cambrex Bio Science), 10% FBS (Gibco; Invitrogen), penicillin (500 U/mL) and streptomycin (100 μg/mL).

The COS and HeLa cell lines and murine endotheliomas (B-end, H-end, E-end) (13) were cultured in DMEM (Cambrex Bio Science), 10% FBS (Gibco; Invitrogen), penicillin (500 U/mL), and streptomycin (100 μg/mL).

Detroit fibroblasts were cultured in DMEM (Cambrex Bio Science), 10% North American serum, penicillin (500 U/mL), and streptomycin (100 μg/mL).

Chicken fibroblasts and mouse embryo fibroblasts were purchased from ATCC (LGC Promochem) and cultured in DMEM, 4.5 g/L glucose, 10% FBS (Gibco; Invitrogen), penicillin (500 U/mL), and streptomycin (100 μg/mL).

U293 cell lines were cultured in Iscove's Modified DMEM (Cambrex Bio Science), 10% FBS (Gibco; Invitrogen), penicillin (500 U/mL), and streptomycin (100 μg/mL).

VSMCs derived from Zucker lean rat aorta and from human arterioles were subcultured until passage number 5 as previously described (14).

Mural Ao cells were extracted as described (15). Briefly, thoracic aortas were excised from E18 chicken embryos, cleaned of fibroadipose tissue, cut into small pieces, and incubated for 5 h at 37 °C in culture medium containing 1.5 mg/mL collagenase (Sigma-Aldrich). The cells isolated from aortas were washed twice in culture medium, plated on a culture dish, and maintained in DMEM (Cambrex Bio Science), 10% FBS (Gibco; Invitrogen), penicillin (500 U/mL), and streptomycin (100 μg/mL), in a humidified incubator at 37 °C until passage 8 (15)

DNA Constructs. A neurexin 1β fusion protein carrying GFP at the C-terminal end was generated by using as template the construct codifying for rat neurexin 1β (pCMVN1b-3) and the pEGFP-N1 vector (Invitrogen).

Rat neurexin 1β was cloned in the third-generation lentiviral vector pCCL.sin.cPPT.PGK.GFP.WPRE (16) for overexpression in primary cells.

The construct pCMVbN1a-1 codifies for *Bos taurus* neurexin 1α and was used to transfect HeLa and COS cells.

The human neurexin 2β construct was synthesized by Gene Art (GeneArt AG). Human neuroligin 1-expressing vector was generated using as template KIAA1070 obtained from the Human Unidentified Gene-Encoded Large Proteins Analyzed (HUGE) database that was cloned in the pCDNA3 vector (Invitrogen).

Gallus gallus neurexin 3β was cloned from chicken embryo arteries by RT-PCR using the Phusion High-Fidelity Kit (Finnzymes) with primers 5′-GTGCCTTGACCATGCACCTGAGAACAAA-3′ and 5′-TTACACATAATACTCTTTGTCCTTGTTTTTCTGTTTC-3′. The corresponding PCR product was first TA-cloned into the pCR2.1TOPO (Invitrogen) and subsequently was subcloned into the pCDNA3 vector (Invitrogen).

Antibody Production. The anti-β-neurexin humanized recombinant antibody (anti-βNRXN, clone AbyD02101) was produced by AbD Serotec MorphoSys-AG, using the HuCALGOLD library (17, 18). The β-specific peptide HF-HGSSKHHSVPIAIYRSPASLRG was used in the screening. The in vivo use of this antibody is restricted and may require a license from MorphoSys AG. Anti-βNRXN was produced with the minimal requirement that it would specifically recognize the β forms of neurexins in native and/or denatured conditions; the optimal result was that it would block some of the activities mediated by β-neurexin. This reagent recognized native β-neurexins but not α-neurexin and was validated in different assays (see *SI Material and Methods* and Fig. S7).

Polyclonal anti-NRXN was produced as whole serum by Elevage Scientifique des Dombes (Charles River Laboratories). Rabbits were immunized with the peptide AKSANKNKKNKDKEYYV, located in the common region of α- and

β-neurexin at the C-terminal tail (Fig. S2). The antibody then was purified from serum by affinity chromatography using the immobilized antigenic peptide at a concentration of 0.2 mg/mL.

Rabbit polyclonal anti-NLGN antibody was produced and purified by New England Peptide through rabbit immunization with PHPHPHSHSTTRV peptide (19). The concentration of this purified antibody was 0.4 mg/mL.

Tissue Immunohistochemistry and Immunofluorescence. Chicken organs (brain, liver, spleen, lung) and adult mouse brain (FVB/n strain) were fixed in Zinc-fix (Becton-Dickinson) or 4% paraformaldehyde (PFA) and embedded in paraffin or frozen in cryostat embedding medium (Killik; Bio-Optica).

Mouse embryos, fixed with Zinc-fix (Becton-Dickinson) and embedded in paraffin, were purchased from Novagen (EMD Biosciences). Adult mouse organs were extracted from BALB/c mice, fixed with Zinc-fix (Becton-Dickinson), and embedded in paraffin.

Human tissues were derived from patients operated at the Institute for Cancer Research and Treatment, Candiolo, Italy, and were provided by the team of L. Capussotti. Healthy liver tissue and liver metastases arising from primary cancer of the colon/rectum were fixed in zinc fix (Becton-Dickinson) and embedded in paraffin.

We prepared 5- to 10-μm tissue sections using standard immunohistochemistry protocol after deparaffinization, when necessary, and rehydration.

Slides were permeabilized in 0.2% Triton X-100 (Sigma-Aldrich), treated for 5–20 min with 3% hydrogen peroxide (Sigma-Aldrich) to quench endogenous peroxidases, and saturated in 10% goat serum (DakoCytomation) for 1 h at room temperature. The tissues were then incubated for 1 h with the primary antibodies diluted in 2.5% goat serum (DakoCytomation), washed 4 times in PBS, and incubated for 40 min with the secondary HRP-conjugate antibody (EnVision; DakoCytomation). The immunochemical reaction was visualized with the AEC kit or DAB kit (DakoCytomation). The tissues were counterstained with Mayer's hematoxylin (Vector Laboratories) and mounted on glass slides.

For staining with the monoclonal anti-αSMA antibody on mouse tissues, the M.O.M kit (Vector Laboratories) was used following the manufacturer's instructions.

For the competitive assays the polyclonal anti-NRXN antibody was preincubated for 30 min with 0.5 μg/μL of either the specific or an unrelated peptide.

In immunofluorescence experiments on mouse and human tissues, the same protocol was applied. Tissue sections were saturated in 10% Donkey serum (Sigma-Aldrich) and 488 or 555 Alexa Fluor secondary antibody (1:200, Invitrogen) was used. Images were analyzed using an inverted fluorescence microscope (DM IRB; Leica) equipped with 63×/1.30 HCX Plan-Apochromat (Carl Zeiss MicroImaging, Inc.) glycerin-immersion objectives.

For the immunofluorescence detection on chicken embryo tissues, some modifications of the standard protocol were applied. Paraffin-embedded tissues were sectioned, deparaffinated, and rehydrated. After permeabilization and endogenous peroxidase quenching, 1 h of saturation was performed in TBS 3% BSA (Fluka, Sigma-Aldrich). The Tyramide Signal Amplification Kit (Molecular Probes; Invitrogen) was used following the manufacturer's instructions. To decrease the blood vessel autofluorescence signal, slides were incubated for 10 min in a 70% ethanol, 0.3% Sudan Black B solution (Sigma-Aldrich), rinsed in TBS, and mounted. Co-localization analysis was performed using a Leica TCS SP2 AOBS confocal laser-scanning microscope (Leica Microsystems).

Immunohistochemistry and immunofluorescence experiments were performed using the following antibodies: mouse anti-αSMA (1:2000, Sigma-Aldrich), rabbit anti-αSMA (1:200; Abcam), rabbit anti-CD31 (1:20; DakoCytomation), rabbit anti-Laminin (1:100; Abcam), rabbit anti-FVIII (1:200; DakoCytomation), mouse or rabbit anti-Flk1 (1:100, sc6251 or sc504;Santa Cruz Biotechnology), rabbit anti-Collagen IV (1:500; Abcam), mouse anti-MAP2 (1:200; Sigma-Aldrich), mouse anti-neurofilament H (1:200; NA1540; LiStarFish), mouse anti-tyrosine hydroxylase (1:200; Chemicon International), rabbit anti-synaptophysin (1:50; Synaptic Systems), mouse anti-SV2 (1:100; Hybridoma Bank, The University of Iowa) mouse anti-NLGN 4F9 (1:100; Synaptic Systems), rabbit polyclonal anti-NLGN (1:100), and rabbit polyclonal anti-NRXN (1:40).

Tissue Immunoprecipitation and Co-Immunoprecipitation. For each experimental point, 25 E18 chicken embryo arteries, 3 E10 CAMs, and half of an E18 chicken embryo brain were used. Frozen tissues were disgregated with a tissue potter and lysed for 40 min in ice with EB buffer (10 mM Tris·HCl, pH 7,5; 150 mM NaCl; 5 mM EDTA, pH 8; 10% glycerol; 1% Triton X-100; and 1% CHAPS) and protease and phosphatase inhibitors (50 μg/mL pepstatin, 50 μg/mL leupeptin, 10 μg/mL aprotinin, 1 mM PMSF, 100 μM $ZnCl_2$, 1 mM Na orthovanadate, and 10 mM NaF). After centrifugation and quantification with the BCA Protein Assay Reagent Kit (Pierce Chemical Co.), samples (6 mg of total proteins from arteries, 4 mg from CAM, and 600 μg from brain for NRXN IP or 6 mg from brain for NLGN IP) were pre-cleared with protein A-Sepharose (Amersham Biosciences) and incubated for 1 h with rabbit anti-NRXN antibody (1.5 μg/mg) or rabbit polyclonal anti-NLGN antibody (2.5 μg/mg). Immune complexes were recovered on protein A-Sepharose for 1.5 h and were washed 4 times. Proteins were separated by 8% SDS/PAGE electrophoresis gel, transferred to polyvinylidene difluoride membrane (Millipore), and detected by immunoblot. For neurexin detection, the membrane was incubated with the mouse monoclonal anti-NRXN antibody (Becton-Dickinson); for neuroligin detection, the membrane was incubated with mouse monoclonal anti-NLGN antibody (4F9; Synaptic Systems). Immunoreactive proteins were identified with an HRP-conjugated secondary antibody (Jackson ImmunoResearch) and visualized by an ECL system (Amersham Biosciences).

For the co-immunoprecipitation experiments, some modifications were applied. A different lysis buffer was set up (20 mM Tris·HCl, pH 7.5; 100 mM NaCl; 20 mM $NaHCO_3$; 4 mM KCl; 2.5 mM $MgCl_2$; 2.5 mM $CaCl_2$; 10% glycerol; 1% Triton X-100; 1% CHAPS) to preserve neurexin–neuroligin interaction. Before standard immunoprecipitation, 6-mg samples of total proteins from arteries and brain were pre-cleared for 2.5 h with rabbit Ig (DakoCytomation) conjugate to protein A-Sepharose for 1 h at 4 °C. In these experiments, a control immunoprecipitation was performed with non-immune rabbit immunoglobulins (DakoCytomation). The co-immunoprecipitated proteins were visualized by immunoblotting, and then the membranes were stripped for the second Western blot detection.

Aortic Ring Assay. Mesenteric arteries were removed surgically from E18 chicken embryos, transferred to a petri dish, and rinsed in PBS. The fibroadipose tissue around the vessels was removed carefully under a stereomicroscope, and artery rings 1 mm in length were cut. Growth factor-reduced Matrigel (Becton-Dickinson) was added to the well of a 48-well plate and then was incubated at 37 °C for 30 min to allow gel formation. The rings were transferred onto Matrigel in each well, covered with 0.2 mL of Matrigel, and incubated at 37 °C for 30 min. The culture was maintained in serum-free MCDB131 medium (Sigma-Aldrich) in a humidified incubator at 5% CO_2 and 37 °C and was stimulated with 10 ng/mL FGF-2 (R&D Systems) and 40 μg/mL of anti-βNRXN antibody or human IgG $Fab_{(2)}$ fragment for 3 days. Sprouting was visualized by observing the specimens in phase contrast with inverted photomicroscope (Leica Microsystems), and 5× magnification images were captured using a digital camera. The sprouted areas were quantified with the ImageJ program (http://rsb.info.nih.gov/ij/). The aortic disk area (A_0) and the total ring area (A_1) were calculated for each ring. The disk area of each ring was subtracted from the total area ($A_1 - A_0 = As$), and the sprouted areas then were expressed as a percentage of the disk area (A_0): $As/A_0 \times 100$.

After 4 days of incubation, samples were fixed for 48 h in zinc fix and were embedded in paraffin.

CAM Assay. Fertilized chicken embryos were incubated for 3 days at 37 °C at 70% humidity. A small hole was made over the air sac at the end of the egg, and a second hole was made directly over the embryonic CAM. After 7 days, cortisone acetate-treated 5 mm filter disks treated with cortisone acetate were saturated with 5 μL of 100 ng/mL FGF-2 (R&D Systems) and 9 μg anti-βNRXN antibody or human IgG $Fab_{(2)}$ fragment (Jackson ImmunoResearch) and were laid on the CAM.

To study the angiogenic activity of neuroligin, 100 μL of Cultrex Basement Membrane Extract (R&D Systems) containing 1×10^6 MDA-MB 435 + PAE-NLGN cells or MDA-MB 435 + PAE-WT were placed on the top of the growing CAM at day 10.

After 2 to 3 days, the disks or Cultrex plugs containing CAMs were fixed with PBS-4% paraformaldehyde for 10 min at room temperature, filter disks or plugs were excised, and pictures were taken with a QIcam FAST1394 digital color camera (QImaging) connected to the stereomicroscope (model SZX9; Olympus).

The angiogenic response was evaluated by counting the vessel branch points on a well-defined and constant area of CAMs using the ImageJ 1.36b program. In neuroligin angiogenesis studies, the assay was performed using 2 different clones of PAE-neuroligin to ensure reproducibility.

The statistical analysis (ANOVA followed by the Student Neuman-Keuls as a multi-comparison test, alpha level of 0.01 or 0.05) was performed using the SPSS 15.0 program.

Protein Immunoprecipitation from Cultured Cells. Confluent ECs were washed 3 times with cold PBS containing 1 mM Na orthovanadate and were lysed in lysis buffer (50 mM Tris·HCl, pH 7.5; 150 mM NaCl; SDS 0.1%, 1% Triton X-100)

and protease and phosphatase inhibitors (50 μg/mL pepstatin, 50 μg/mL leupeptin, 10 μg/mL aprotinin, 1 mM PMSF, 100 μM $ZnCl_2$, 1 mM Na orthovanadate, and 10 mM NaF) for 30 min. After centrifugation (30 min at 11,000 $\times$ *g*), the supernatant was quantified with the BCA Protein Assay Reagent Kit (Pierce Chemical Co.). Then 1 mg of protein was pre-cleared by incubation for 1.5 h with protein A-Sepharose (Amersham Biosciences) and incubated for 1 h with 1 μg/mg of mouse anti-NLGN (clone 4F9; Synaptic Systems) or 2 μg/mg of polyclonal anti-NRXN. The immune complexes were recovered on protein A-Sepharose for 1.5 h; beads were washed 4 times and bound proteins were detected by immunoblot. Proteins were separated by 8% SDS/PAGE electrophoresis gel, transferred to polyvinylidene difluoride membrane (Millipore), incubated with mouse anti-NLGN 4F9 (1:1000; Synaptic Systems) or monoclonal anti-NRXN (1:250, Becton-Dickinson) and HRP-conjugated secondary antibody (Jackson ImmunoResearch), and were visualized by an ECL system (Amersham Biosciences).

Immunofluorescence Analysis. COS cells were transfected with pCMVN1b-3, for transient neurexin 1β expression, using the Lipofectamine Plus reagent (Invitrogen) according to the manufacturer's instructions. Cells were plated onto gelatin-coated glass coverslips in 24-well plates and left to adhere. After MetOH fixation for 10 min at -20 °C, coverslips were blocked with 2% BSA (Fluka; Sigma-Aldrich). The staining was performed with 5 μg/mL of recombinant anti-βNRXN antibody and 3 μg/mL of anti-human Fab Cy-3 (Jackson ImmunoResearch) in 0.2% BSA (Fluka, Sigma-Aldrich). DAPI (Molecular Probes; Invitrogen) nuclear staining was added to the secondary antibody solution. Coverslips were mounted and analyzed using an inverted fluorescence microscope (DM IRB; Leica).

FACS Analysis. FACS experiments were performed with the neurexin 1β-GFP PAE clone or HeLa cells transiently transfected with pCMVN1b-3 (*Rattus Norvegicus* neurexin 1β), pCDNA3.1 (*Homo sapiens* neurexin 2β), pCDNA3 (*Gallus gallus* neurexin 3β), and pCMVbN1a-1 (neurexin 1α) constructs. Cells were harvested in PBS 2 mM EDTA (Sigma-Aldrich), and 2 $\times$ 10^5 cells/point were saturated in 1% BSA (Fluka; Sigma-Aldrich). Next, the recombinant anti-βNRXN antibody (2.5 μg/mL) or human IgG $Fab_{(2)}$ fragment (Jackson ImmunoResearch) was incubated for 30 min on ice and, after 3 washes, 2.5 μg/mL of R-phycoerythrin–conjugated anti-human Fab antibody (Jackson ImmunoResearch) was incubated for 30 min.

For competitive assay, the antibodies were preincubated with 1 μM of specific or 10 μM of unrelated peptides for 30 min.

After the final washes in 1% BSA (Fluka; Sigma-Aldrich), samples were fixed in 2% paraformaldehyde and analyzed by FACScan (Becton Dickinson).

Haptotaxis. Ao-neurexin 1β cells and Ao-control vector cells were pretreated for 1 h with 10 μg/mL of anti-βNRXN antibody or human IgG $Fab_{(2)}$. Then 5 $\times$ 10^4 cells/well were seeded in serum-free medium on the upper side of 8-μm pore filters in Transwell chambers (Costar). On the lower side, the filters were coated with 25 μg/mL laminin (from Engelbreth-Holm-Swarm murine sarcoma; Sigma-Aldrich). The lower compartment of the chamber was filled with serum-free medium with 20 ng/mL FGF-2 (R&D Systems). After 5 h of incubation at 37 °C, 5% CO_2, cells on the upper side of the filters were mechanically removed, and those that had migrated to the lower side of the filters were fixed in 2.5% glutaraldehyde for 30 min and stained with 0.1% crystal violet. For each sample, 4 random fields on the lower surface of the filters were counted at 10$\times$ magnification.

Adhesion Assay. For the adhesion assay, 96-well plates (Costar) were coated for 1 h with 5 μg/mL of collagen (Sigma-Aldrich) or 15 μg/mL of laminin (from Engelbreth-Holm-Swarm murine sarcoma; Sigma-Aldrich) and then were saturated with a solution of PBS 3% BSA (Fluka; Sigma-Aldrich). Ao-neurexin 1β, Ao-control vector, or Ao-WT was collected and pretreated with 10 μg/mL of anti-βNRXN antibody or human IgG $Fab_{(2)}$ fragment for 1 h; 2 $\times$ 10^4 cells/plate were allowed to adhere for 30 min at 37 °C.

Samples were rinsed in PBS, fixed for 30 min in 8% glutaraldehyde, and stained with 20% methanol, 0.1% crystal violet in PBS. Cells were photographed with a QIcam FAST1394 digital color camera (QImaging) and counted using Image-ProPlus 6.2 software (Media Cybernetics).

Proliferation. Ao-neurexin 1β, Ao-control vector, and Ao WT cells were plated on 48-well plates (Costar), 3,800cells/well, and were allowed to adhere overnight. The cells were stimulated for 72 h with different treatments: DMEM 1% FBS, DMEM 10% FBS, or DMEM 1% FBS plus FGF-2 20 ng/mL (R&D Systems) with 10 μg/mL of anti-βNRXN antibody or human IgG $Fab_{(2)}$ fragment.

Samples were rinsed in PBS, fixed for 30 min in 8% glutaraldehyde , and stained with 20% methanol 0.1% crystal violet for 30 min. The dye was solubilized in 10% acetic acid, and absorbance at 595 nm was evaluated in a multiplate reader.

Survival. Evaluation of the effect of neurexin 1β on cell viability after serum deprivation was assessed by ATP content luminescent assay (ATPligt kit; PerkinElmer) following the manufacturer's instructions and was evaluated in a multiplate reader. Ao-neurexin 1β, Ao-control vector, and Ao-WT cells were plated on 48-well plates (Costar) at 20,000 cells/well and were allowed to adhere overnight. The cells then were stimulated for 72 h by treatment with DMEM 1% FBS, serum-free DMEM, or serum-free DMEM plus 20 ng/mL FGF-2 (R&D Systems) with 10 μg/mL of anti-βNRXN antibody or human IgG $Fab_{(2)}$ fragment.

Aggregation Assay. The aggregation assay was performed with PAE clones overexpressing neurexin 1β-GFP and neuroligin 1. Equal amounts of both cell types were used to reach a final concentration of 1 $\times$ 10^5cells/point in serum-free Ham's F12 medium containing 2 mM $CaCl_2$ or 2 mM EGTA. The cell mixture was incubated at room temperature under gentle mixing; 40 μg/mL of recombinant anti-βNRXN antibody was added before aggregation for 30 min. The number of aggregates was evaluated by phase-contrast observation under an inverted microscope (DM IRB; Leica).

Spheroid Co-Culture. HUVEC and NDHF cells were co-cultured as spheroids as described previously (20). Briefly, 2,500 HUVEC and NHDF cells per spheroid were mixed in a 1:1 ratio in Methocel (Fluka; Sigma-Aldrich), were seeded into nonadhesive round-bottomed 96-well plates, and were allowed to form spheroids for 24 h. The same ratio of cells was cultured on gelatin-coated tissue-culture dishes. After 24 h, spheroids and cultured cells were recovered and washed in PBS, and total RNA was extracted.

Sequence Analysis. The coding sequences of genes were retrieved from the public genome databases NCBI (http://www.ncbi.nlm.nih.gov/entrez/query.fcgi?CMD = search&DB = nucleotide) or Ensembl (http://www.ensembl.org/index.html). Different tools of Ensembl and the EST database of NCBI were used to assemble *in silico* the uncloned coding sequences. The following *Gallus gallus* coding sequences were deposited in NCBI GenBank: neurexin 1β precursor (EU702427), neurexin 3α precursor (EU702428), neurexin 3β precursor (EU702430), and neurexin 3β arterial isoform (EU702429). The primers for GgNLGN2 analysis were designed using the GgEST 24465120 (gi: 50275503).

The DNA or amino acid sequence alignments were performed with a Vector NT 10 (Invitrogen) suite using the ClustalW algorithm (Thompson et al., 1994).

RNA Extraction and RT-PCR. The total RNA was extracted from confluent cell cultures or frozen chicken tissues using the phenol-chloroform method (TRIZMA; Sigma-Aldrich), was treated with DNase-free kit (Ambion; Applied Biosystems), and was quantified with a spectrophotometer (PerkinElmer) or Agilent 2100 Bioanalyzer (Agilent Technologies).

We retrotranscribed 500 ng of mRNA in 20 μL of master mix with or without enzyme (RT SuperScript II; Invitrogen). Then 2 μL of cDNA were amplified in 42 PCR cycles with Taq platinum enzyme (Invitrogen). After the initial denaturation for 12 min at 95 °C, the cycles consisted of 30 s at 94 °C, 1 min of an annealing step specific for each primer, and 30 s at 72 °C. A final cycle of 12 min at 72 °C was performed. The PCR products were separated in a 2% agarose gel and were sequenced. The following list is a summary of the primers used, organized by species. For each primer we give the information in this order: target gene, melting temperature (in °C), sequence (5′-3′ forward, reverse), PCR product length (in bp):

GgNRXN1α; 56; GACTTGCCAAGCAAGGAGAC, TGAATTTCAGCCATCTGTCG; 628

GgNRXN1β; 56; ATTTCCACGGCAGCAGCAAA, ACCAGAGAGCTGGCCTTGGA; 611

GgNRXN3α; 56; ACAGTGCTAGTGCTGGATGGTGAA, AGCCCAGCATTGTGTAGTCTTCCT; 1186

GgNRXN3β; 56; TGTGGAGTTCCTCTAACGTGGCTT, CACCCAAGTGGGAATCCAAGGACTTT; 1361

GgNLGN1; 56; AGAAGGCAGGTTGCCTGAAGTCAT, GCTGGTTGAATGTCCTGGTCAACA; 804

GgNLGN2; 56; C ATCTCCAGCTGGTCGGTCAACTA, ACATGAACTTGATGGTCTCCCGCA; 356

GgNLGN3; 56; TGCCCATCTGGTTTACCTCCAACT, AAGGCGATGTTCTCACTGACCCAA; 346

GgNLGN4; 56; CCCAATGAAATCCTTGGTCCAGTG, CTGAGGGTCATCTGGAATCACATCTC; 1002

MmNLGN1; 60; ACTCAGTTTGCTCCTGTATGTCCC, ATGTTCTCGCTGGTCCATCTTAGG; 464

MmNLGN2; 60; ATGTCATGCTCAGCGCAGTA, ACTGCCACAGTCACGCTTAG; 469

MmNLGN3; 60; ATCGTCGCCACTTATATCCAGGAG, TGTAAGGAGACTGACACAGGATGC; 450

MmNRXN1; 58; CAGCAAGCATCATTCAGTGCCT, CTATGGCGATGTTGGCATCGTT; 559

MmNRXN2; 58; ATCAACCGCATGCCCTTCCTCA, TTGTAGTAGAGGCCGGACACCT; 581

HsNLGN1; 60; AAGACCAGAGCGAAGACTGCCTAT, GGTCCCAAACCAGTGATGGTGTAT; 481

HsNLGN2; 60; GTGCGCAACGCCACCACCCT, GAGCCAGCGCAGGGCCTGGATCT; 450

HsNLGN3; 60; ACAGCTGTGCCCGAAGTCAT, ATGCCCGAGCCAAAGACAGT; 473

HsNLGN4; 60; GGCGGTTTCAGCCACCAGAA, CCGCCAAAGGCTCCGACATT; 472

HsNRXN1; 55; CAGCAAGCATCATTCAGTGCCT, CTATGGCGATGTTGGCATCGTT; 559

HsNRXN2; 55; ATCAACCGCATGCCCTTCCTCA, TTGTAGTAGAGGCCGGACACCT; 581

HsNRXN3; 55; ATTGGCACAGTTGACATCTCCATC, TCATGGACAGGGAATCTTTGGTGG; 673

For the screening of PAE cells, different primers were tested because of the high conservation of the neurexin and neuroligin sequences between species. The primers MmNRXN1, HsNLGN1, and HsNLGN2 amplified the porcine genes. HsNRXN3 primers were used for neurexin 3 amplifications from mouse embryo fibroblasts.

Taqman Low-Density Array. Single-strand cDNA synthesis from total RNA was prepared using TaqMan reverse transcription reagents (Applied Biosystems) as recommended by the manufacturer. TaqMan assays were purchased from Applied Biosystems for the selected genes: angiopoietin 1 (ANGPT1, Hs00375822_m1), angiopoietin 2 (ANGPT2, Hs00169867_m1), caldesmon 1 (CALD1, Hs00263989_m1), calcium/calmodulin-dependent serine protein kinase (CASK, Hs00177620_m1), discs large homolog 1 (DLG1, Hs00177739_m1), discs large homolog 4 (DLG4, Hs00176354_m1), neuroligin 1 (NLGN1, Hs00208784_m1), neuroligin 2 (NLGN2, Hs00793093_m1), neuroligin 4 Y-linked (NLG4Y, Hs00382154_m1), neurexin 2 (NRXN2, Hs00373339_m1), neurexin 3 (NRXN3, Hs00191244_m1), platelet-derived growth factor receptor β (PDGFRB, Hs00182163_m1), transforming growth factor β 1 (TGFB1, Hs99999918_m1), hypoxanthine phosphoribosyltransferase 1 (HPRT, Hs99999909_m1).

Each qPCR reaction performed was normalized to the endogenous HPRT. All qPCR analyses were performed in duplicate with ABI PRISM 7900 HT Fast Real-Time PCR system (Applied Biosystems). The raw data were analyzed using SDS2.2 (Applied Biosystems) and expressed as relative quantity (RQ).

Contractile Response in Embryonic Chicken Mesenteric Artery. After the dissection, the vessels (length 1.5–2 mm; intraluminal diameter 546.9 $\pm$ 72.5 μm, $n = 18$) were incubated in DMEM alone, in 20 μg/mL of human IgG $Fab_{(2)}$, or in 20 μg/mL of anti-βNRXN antibody and were maintained in culture ON at 37 °C. Arterial rings were mounted in a wire myograph in physiological saline solution (PSS; composition: 118 mM NaCl; 4.6 mM KCl; 23 mM $NaHCO_3$; 1.2 mM $MgSO_4$; 1.2 mM KH_2PO_4; 1.2 mM $CaCl_2$; 10 mM glucose; 0.025 mM EDTA, pH 7.4, at 37 °C) aired with 95% O_2-5% CO_2, and maintained at 37 °C. The normalized passive resting force and the corresponding diameter then were determined for each preparation from its individual length–pressure curve. In brief, individual resistance vessels were mounted on 2 100-μm wires in the jaws of the myograph and were bathed in 5 mL of PSS. The tension at which the vessel is held has a direct relationship with the response to test agonists. The vessels therefore were held at a standardized tension of 100 mm Hg to mimic mean arterial blood pressure. Length–tension curves were obtained with the LabVIEW (National Instruments, Austin, TX) software, and normalization of the vessels to physiological tension was performed by distending the vessel in stepwise fashion on the myograph and recording changes in tension readings on the digital display. The *Pi* (effective pressure) of the vessel was calculated by the law of Laplace. When a resting tension of 100 mm Hg was achieved, the jaws were held in this position for the duration of the experiment, and the vessels were left in PSS to equilibrate for 20 min after the tension was set before experimentation. Subsequent responses were recorded as changes in tension transmitted through the myograph force transducer. After normalization and 20-min equilibration in PSS, the preparations were stimulated with isotonic depolarizing KCl solutions in which part of the NaCl had been replaced by an equimolar amount of KCl (composition: 22.6 mM NaCl; 98.8 mM KCl; 25 mM $NaHCO_3$; 1.2 mM $MgSO_4$; 1.2 mM KH_2PO_4; 1.2 mM $CaCl_2$; 10 mM glucose; 0.025 mM EDTA, pH 7.4, at 37° C) to test the viability of the vessel. The arterial rings then were incubated with PSS alone, 20 μg/mL of human IgG Fab (2), or 20 μg/mL of anti-βNRXN antibody for 30 min. Cumulative dose–response curves to NA (0.01–100 μM) were performed, and the force generated was expressed as wall tension (calculated by dividing the force by 2 times the length of the vessel segment). Maximal response values (E_{max}) were calculated from the respective dose–response equations obtained by nonlinear regression analysis.

1. Glebova NO, Ginty DD (2005) Growth and survival signals controlling sympathetic nervous system development. *Annu Rev Neurosci* 28:191–222.
2. Vaucher E, Tong XK, Cholet N, Lantin S, Hamel E (2000) GABA neurons provide a rich input to microvessels but not nitric oxide neurons in the rat cerebral cortex: A means for direct regulation of local cerebral blood flow. *J Comp Neurol* 421(2):161–171.
3. Nicosia RF, Ottinetti A (1990) Growth of microvessels in serum-free matrix culture of rat aorta. A quantitative assay of angiogenesis in vitro. *Lab Invest* 63(1):115–122.
4. Kilarski WW, Jura N, Gerwins P (2005) An ex vivo model for functional studies of myofibroblasts. *Lab Invest* 85(5):643–654.
5. Nguyen T, Sudhof TC (1997) Binding properties of neuroligin 1 and neurexin 1beta reveal function as heterophilic cell adhesion molecules. *J Biol Chem* 272(41):26032–26039.
6. Hao H, Gabbiani G, Bochaton-Piallat ML (2003) Arterial smooth muscle cell heterogeneity: Implications for atherosclerosis and restenosis development. *Arterioscler Thromb Vasc Biol* 23(9):1510–1520.
7. Thyberg J, Blomgren K, Hedin U, Dryjski M (1995) Phenotypic modulation of smooth muscle cells during the formation of neointimal thickenings in the rat carotid artery after balloon injury: An electron-microscopic and stereological study. *Cell Tissue Res* 281(3):421–433.
8. Campbell GR, Campbell JH (1990) The phenotypes of smooth muscle expressed in human atheroma. *Ann N Y Acad Sci* 598:143–158.
9. Gittenberger-de Groot AC, DeRuiter MC, Bergwerff M, Poelmann RE (1999) Smooth muscle cell origin and its relation to heterogeneity in development and disease. *Arterioscler Thromb Vasc Biol* 19(7):1589–1594.
10. Hirschi KK, Rohovsky SA, D'Amore PA (1998) PDGF, TGF-beta, and heterotypic cell–cell interactions mediate endothelial cell-induced recruitment of 10T1/2 cells and their differentiation to a smooth muscle fate. *J Cell Biol* 141(3):805–814.
11. Lawrence JB, Singer RH (1986) Intracellular localization of messenger RNAs for cytoskeletal proteins. *Cell* 45(3):407–415.
12. Deregibus MC, Buttiglieri S, Russo S, Bussolati B, Camussi G (2003) CD40-dependent activation of phosphatidylinositol 3-kinase/Akt pathway mediates endothelial cell survival and in vitro angiogenesis. *J Biol Chem* 278(20):18008–18014.
13. Bocchietto E, et al. (1993) Proliferative and migratory responses of murine microvascular endothelial cells to granulocyte-colony-stimulating factor. *J Cell Physiol* 155(1):89–95.
14. Doronzo G, et al. (2004) Insulin activates vascular endothelial growth factor in vascular smooth muscle cells: Influence of nitric oxide and of insulin resistance. *Eur J Clin Invest* 34(10):664–673.
15. Ray JL, Leach R, Herbert JM, Benson M (2001) Isolation of vascular smooth muscle cells from a single murine aorta. *Methods in Cell Science* 23(4):185–188.
16. Amendola M, Venneri MA, Biffi A, Vigna E, Naldini L (2005) Coordinate dual-gene transgenesis by lentiviral vectors carrying synthetic bidirectional promoters. *Nat Biotechnol* 23(1):108–116.
17. Knappik A, et al. (2000) Fully synthetic human combinatorial antibody libraries (HuCAL) based on modular consensus frameworks and CDRs randomized with trinucleotides. *J Mol Biol* 296(1):57–86.
18. Rothe C, et al. (2008) The human combinatorial antibody library HuCAL GOLD combines diversification of all 6 CDRs according to the natural immune system with a novel display method for efficient selection of high-affinity antibodies. *J Mol Biol* 376(4):1182–1200.
19. Ichtchenko K, Nguyen T, Sudhof TC (1996) Structures, alternative splicing, and neurexin binding of multiple neuroligins. *J Biol Chem* 271(5):2676–2682.
20. Kunz-Schughart LA, et al. (2006) Potential of fibroblasts to regulate the formation of 3-dimensional vessel-like structures from ECs in vitro. *Am J Physiol Cell Physiol* 290(5):C1385–1398.
21. Thompson JD, Higgins DG, Gibson TJ (1994) *Nucleic Acids Res* 22:4673–4680.

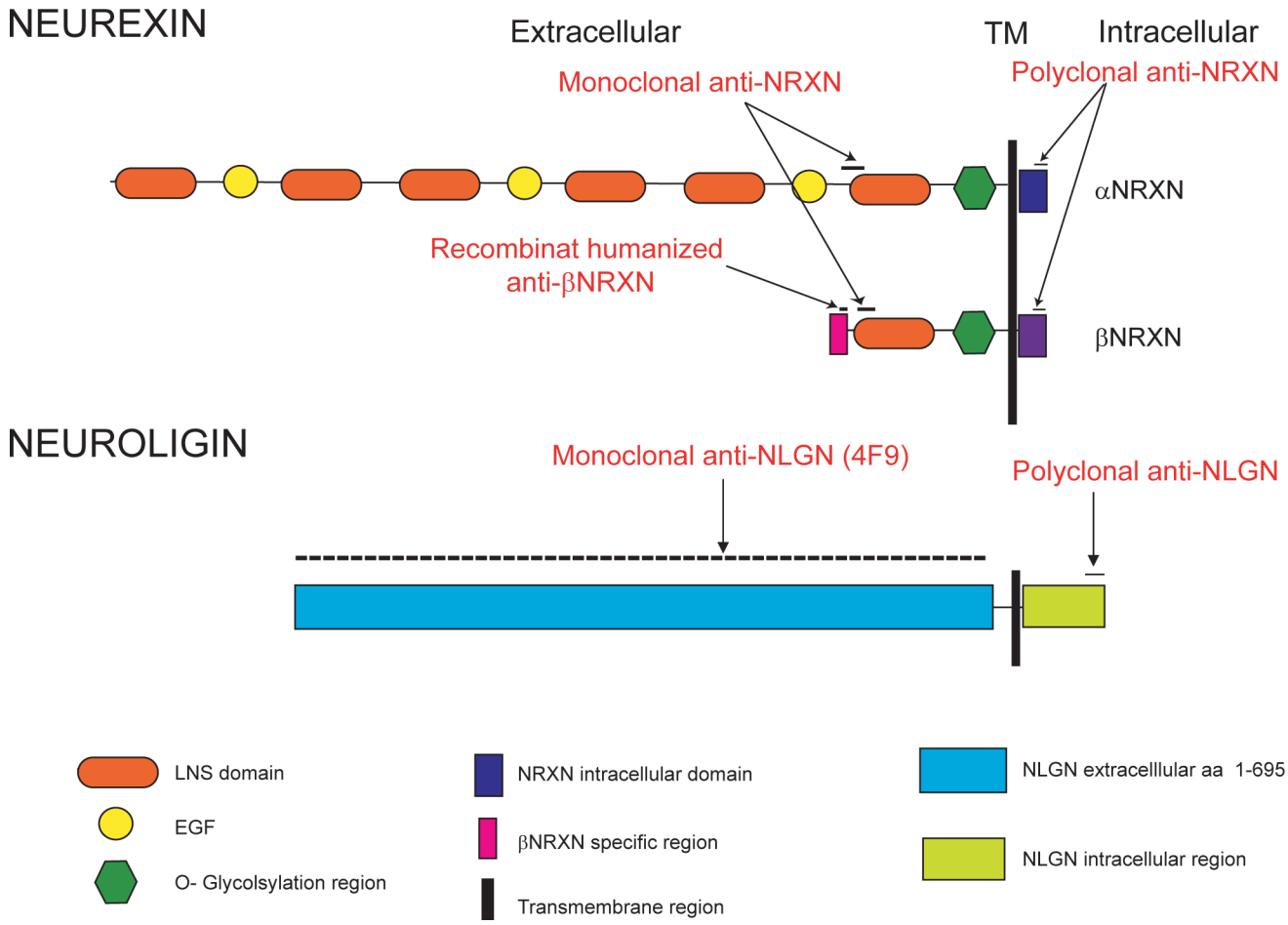

Fig. S1. Schematic representation of the neurexin and neuroligin domain structure. Indicated are the approximate regions recognized by the antibodies used in this project. Drawings are not to scale.

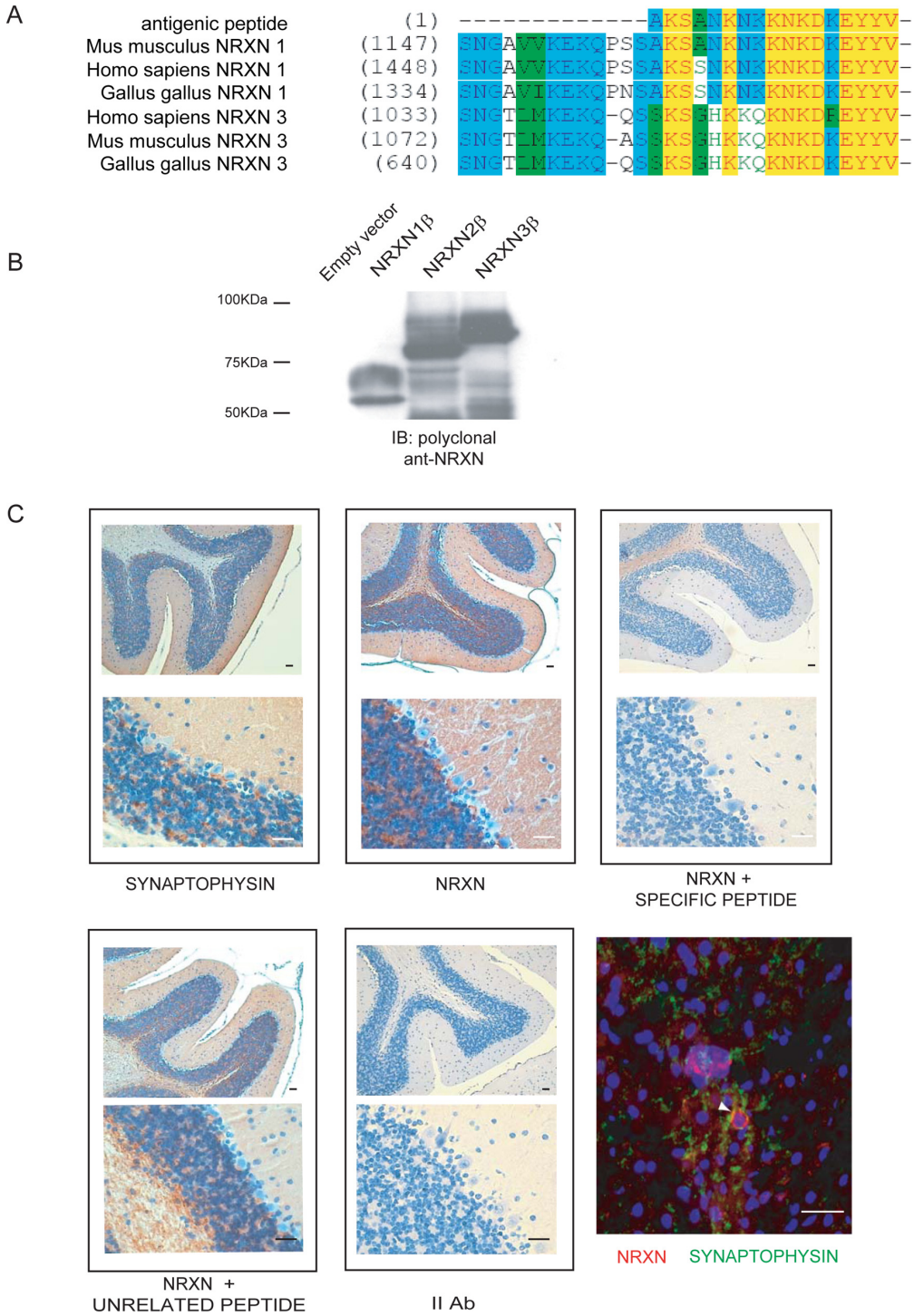

Fig. S2. Characterization of polyclonal anti-NRXN antibody. (*A*) Antigen conservation between different species. Alignment of the antigenic peptide used to raise the polyclonal anti-NRXN antibody shows a high sequence conservation with the C-terminus of *Mus musculus*, *Gallus gallus*, and *Homo sapiens* neurexins. (*B*) Anti-NRXN antibody recognizes all the neurexin isoforms. The polyclonal anti-NRXN antibody recognized neurexin 1β, neurexin 2β, and neurexin 3β in immunoblotting of transfected HeLa cells. This blot shows the molecular weight that could be reached by the neurexin 3β gene products. (*C*) Staining of brain sections by the polyclonal anti-NRXN. Adult mouse sagittal cerebellar sections were stained with the synaptic marker anti-synaptophysin, with the polyclonal anti-NRXN antibody (alone or in combination with the specific or an unrelated peptide), or with the secondary antibody alone. In the granular layer the same cells stained by anti-synaptophysin are recognized by the polyclonal anti-NRXN antibody. The lower right panel represents an immunofluorescence analysis on an adult mouse brain section. The arrowhead indicates a cell body stained identically by the antibodies against synaptophysin (*green*) and neurexin (*red*). (Scale bars, 50 μm)

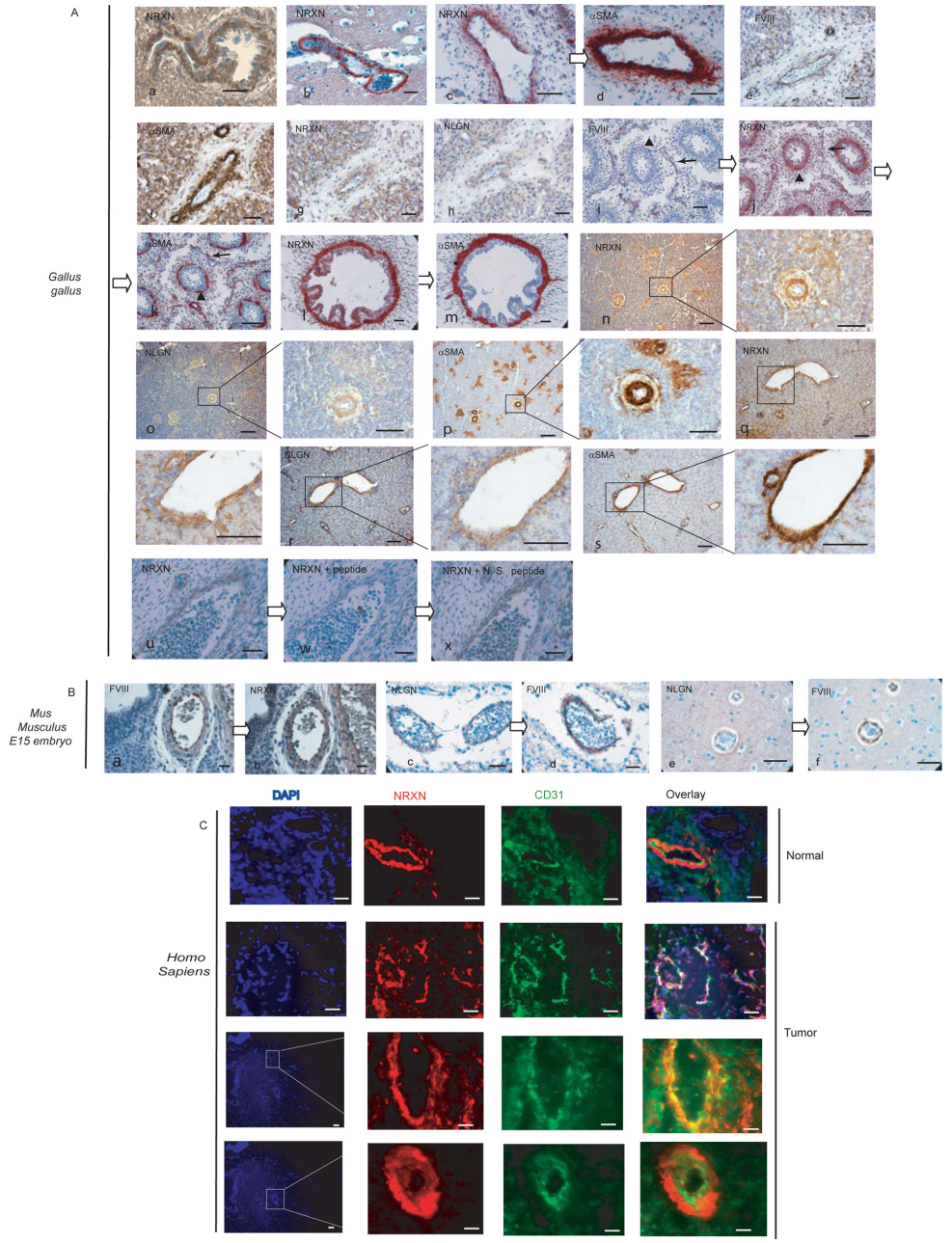

Fig. S3. Wide expression of neurexin and neuroligin in the vascular system. (*A*) Staining of 2 arterioles (*a*, *b*) in a adult chicken brain section in which polyclonal anti-NRXN labeled the blood vessel wall in addition to the surrounding neuronal tissue. (*c*–*h*) Immunostaining performed on sections of E18 chicken embryo lung shows that in different vessels regions of neurexin, α-SMA, and neuroligin expression overlap. Moreover, polyclonal anti-NRXN antibody (*j*) stains both capillaries (*arrow*) and a ring of SMC that surrounds the alveolus (*arrowhead*). The same structures are stained by α-SMA (*k*), whereas anti-FVIII (*i*) antibody stains only the capillaries. A higher magnification of the alveolar SMC stained with anti-NRXN (*l*) and anti- α-SMA (*m*) antibodies is shown also. (*n*–*s*) Low- and high-magnification images of consecutive sections from E18 chicken embryo spleen (*n*–*p*) or liver (*q*–*s*) in which anti-NRXN, NLGN, and α-SMA stain a number of vessels of different sizes in a similar pattern. The liver, spleen, and lung images are representative of an analysis performed on 6 organs extracted from chicken embryos. (*u*–*x*) A section of the chicken embryo (E5) aorta was stained with polyclonal anti-NRXN antibody alone (*u*) or was preincubated with the specific (*w*) or unrelated (*x*) peptides. (*B*) Staining of E15 mouse embryo performed with antibodies to FVIII (*a*, *d*), neurexin (*b*), and neuroligin (*c*) shows the localization of these proteins in the vascular wall. Neuroligin expression in a mouse adult brain section (*e*) was detected in the nerve tissues and, in the vascular wall, in a region overlapping with the FVIII staining (*f*). (*C*) An immunofluorescence analysis performed on human normal liver sections (*Top Row*) or liver metastatic tissue sections (*3 Lower Rows*) with an antibody against the endothelial marker CD31 (*green*), or the polyclonal anti-NRXN (*red*) shows that blood vessels produce neurexin. Images of consecutive sections are linked by an arrow. (Scale bars, 50 μm)

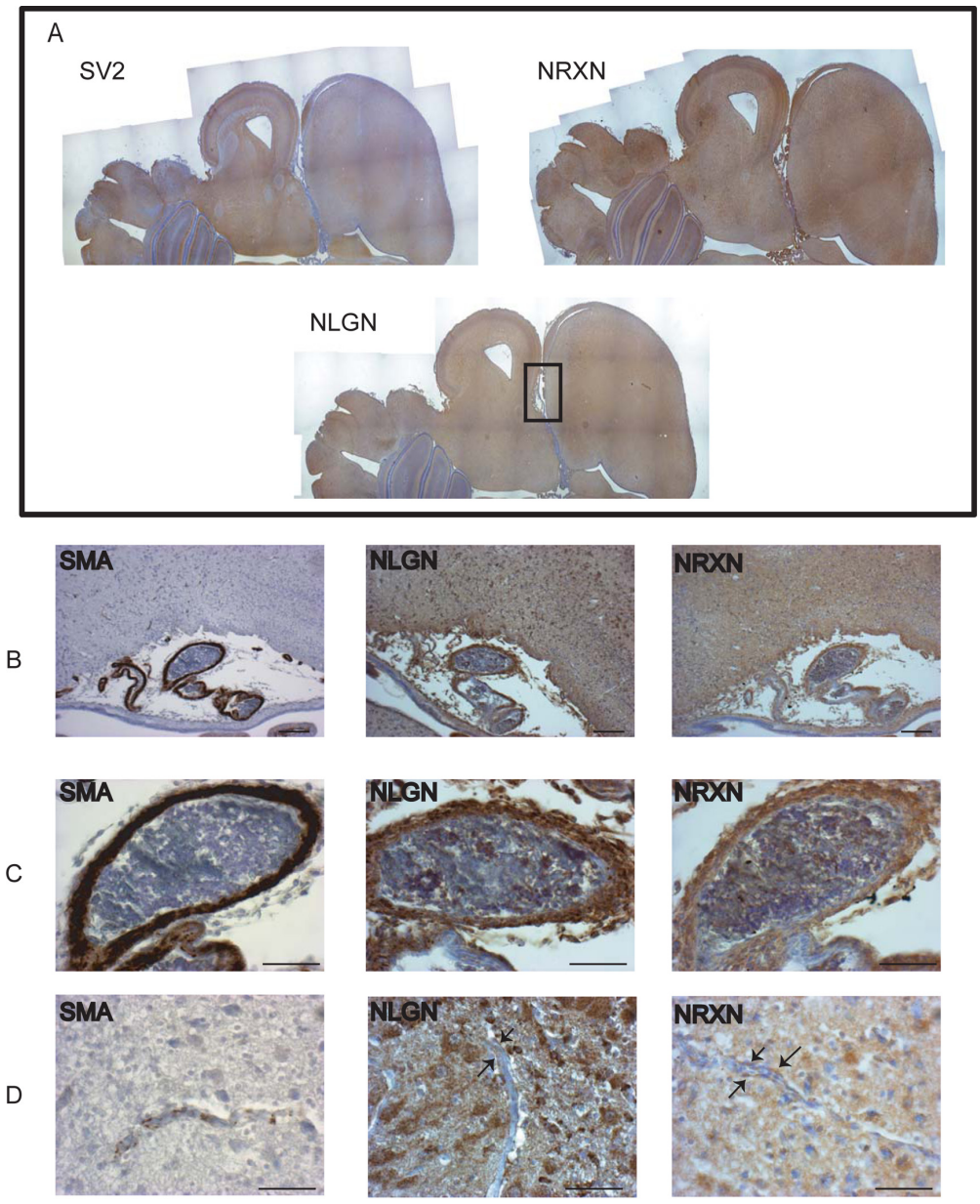

Wall thickness (α−SMA) range μm	Signal Intensity				
	α−SMA	NLGN		NRXN	
		EC	SMC	EC	SMC
5-22 (n=12)	+++	+++	+++	+++/++	+++/++
2-5 (n=8)	++	++		+++/++	
1-2 (n=8)	+	+		+	

Fig. S4. Neurexin and neuroligin expression in whole E18 chicken embryo brain. (*A*) The 3 panels were produced by merging several low-magnification images taken from a region of a horizontal section of an E18 chicken embryo brain. Telencephalon, midbrain, cerebellum, and a part of hindbrain are visible. The labeling of anti-SV2,- NRXN, and -NLGN antibodies shows similar patterns in the whole brain. Several extra-parenchymatic vessels are visible in the region between the telencephalon and the optical lobe (*Lower Panel, Box*). (*B*) High magnification of the boxed area in *A* show the expression of neurexin, neuroligin, and α-SMA in consecutive sections. (Scale bar, 100 μm.) (*C*) Detailed pictures of a large vessel from the region presented in *B*. (Scale bar, 50 μm) (*D*) Examples of neurexin and neuroligin expression in the small vessels that enter the brain parenchyma. In this case the evaluation of neurexin and neuroligin expression is difficult because of the strong expression of these proteins by neurons, but we could find different examples of labeled vessels. The neurexin/neuroligin labeling is indicated by arrows. (Scale bar, 50 μm)

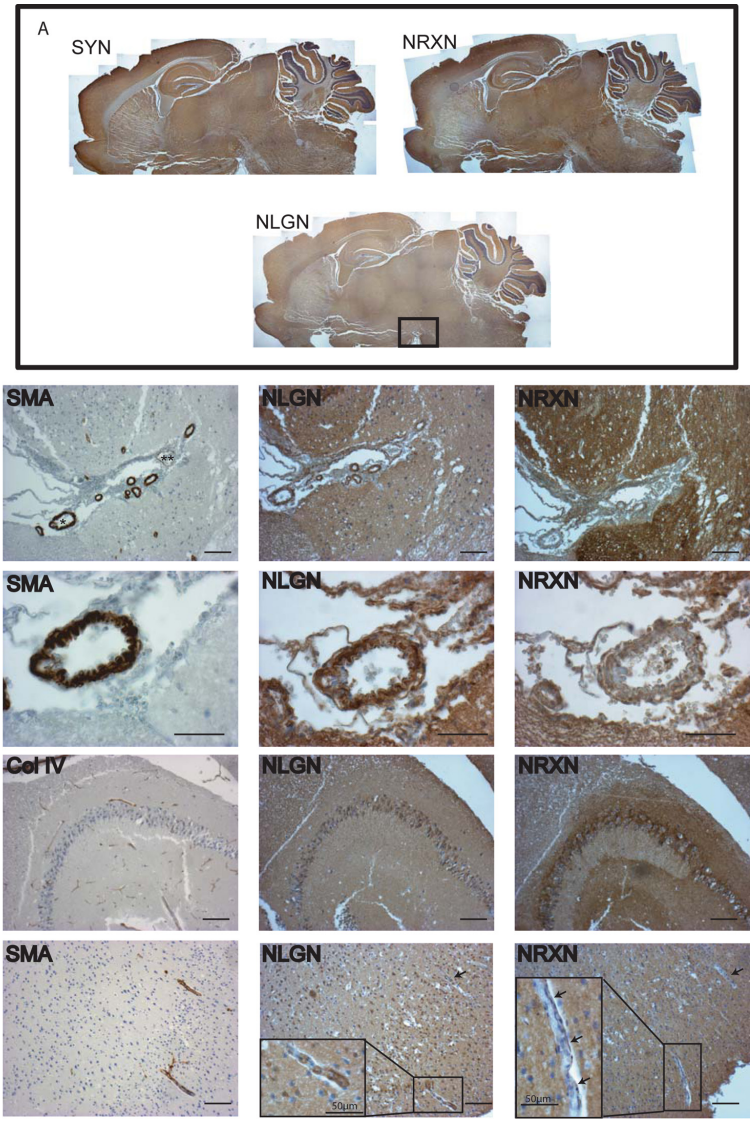

Wall thickness (α−SMA) range μm	Signal intensity				
	α−SMA	NLGN		NRXN	
		EC	SMC	EC	SMC
7-24 (n=12)	+++	+++	+++	-	++
7-12 (n=7)	++	++	++	-	+
4 -7(n=5)	+	++		+	

Fig. S5. Neurexin and neuroligin expression in the whole adult mouse brain. (*A*) The 3 panels were produced by merging several low-magnification images taken from a sagittal section of a mouse brain stained with antibodies to synaptophysin, neurexin, and neuroligin, which produce similar expression patterns. Enriched areas for neurexin and neuroligin expression are located in the cortex, hippocampus, hypothalamus, and cerebellum. (*B*) Magnifications of an area proximal to the hypothalamus (boxed area in *A*), which presents many large vessels, including arteries and veins. An artery (*) and vein (**) are highlighted. (Scale bar, 100 μm) (*C*) High magnifications to show neurexin and neuroligin expression in an artery. Neuroligin is expressed in the entire vascular wall, whereas neurexin is detected in the outer layer of the wall, in a subset of α-SMA-/neuroligin-expressing cells. (Scale bar, 50 μm) (*D*) Representation of an area of the hippocampus. The basal membranes of capillaries are marked by collagen IV. Analysis of neurexin and neuroligin expression in capillaries is hampered by the strong expression of these proteins by neurons. (Scale bar, 100 μm) (*E*) Images showing α-SMA–positive vessels entering the cortical layers of the brain. Neurexin and neuroligin staining again is hampered by the surrounding nerve labeling, but examples of stained vessels are highlighted by arrows and magnifications within the insets. (Scale bar, 50 μm) (*Table*) Evaluation of the levels of neurexin and neuroligin expression in different vessels (from an average of 5 regions representative of 6 brains). Vessels were separated into 3 classes depending on the thickness of the α-SMA staining in their walls. Arbitrary expression levels are as follows: +++, strong; ++, good; +, weak. Separation between ECs and SMCs cells is provided for the first 2 classes. The class of blood vessels with an α-SMA wall width in the range of 7–24 μm contains many arteries in which the neurexin staining is restricted to a subset of SMCs in the wall. An example is presented in *C*. The class of blood vessels with an α-SMA wall width in the range of 7–12 μm contains mostly veins.

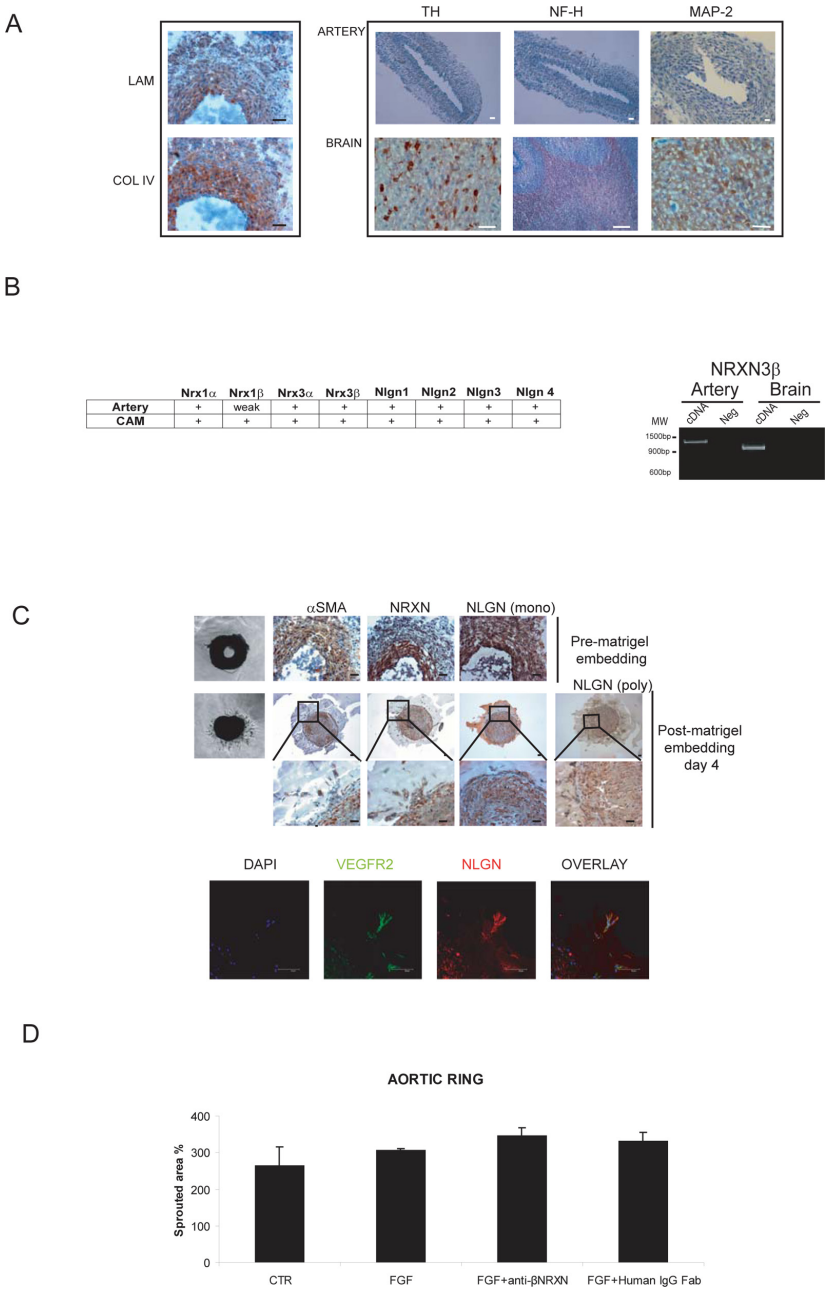

Fig. S6. Expression of neurexin and neuroligin isoforms in chicken arteries and CAM, artery ring characterization, sprouting, and the effect of the anti-βNRXN antibody. (*A*) Immunohistochemical characterization of E18 chicken embryo arteries for basal membrane and nerve marker expression. (*Left*) Laminin (LAM) and collagen IV (COL IV) signals were diffuse throughout the vascular wall, indicating that the basal lamina is not well formed in these vessels. The nerve markers tyrosine hydroxylase (TH), neurofilament-H (NF-H), and microtubule-associated protein 2 (MAP2) stained the chicken brain (*Bottom Row*) but did not stain the artery (*Top Row*), demonstrating that no nerve tissue was collected in the samples of chicken arteries. (Scale bar, 50 μm) (*B*) (*Top*) RT-PCR analysis of the expression of neurexin and neuroligin isoforms in chicken embryo tissues. All the neurexin and neuroligin isoforms are expressed in CAM and embryonic arteries. (*Bottom Left*) The table summarizes the analysis of expression during different developmental stages. The neurexin 2 gene is not cited because we could not isolate this coding sequence from the *Gallus gallus* genome. (*Bottom Right*) The PCR product analysis of the neurexin 3β gene in chicken embryo. Neurexin 3β is transcribed as a longer form in the artery than in brain. (*C*) Immunohistochemical staining of arteries before and after sprouting in Matrigel. Phase-contrast images are representative of an artery ring before and after sprouting in Matrigel. Cells expressing α-SMA, neurexin, and neuroligin are completely relocated from a discrete number of SMC concentric rings (*Top Row*) to a scattered pattern (*Middle Row*) in arteries after 4 days of sprouting in Matrigel. The sprouting artery was stained with both the monoclonal (mono) and the polyclonal (poly) anti-NLGN antibodies. (Scale bar, 50 μm) The bottom row presents a sprouted area of the ring in which NLGN1 (*red*) and VEGFR2 (*green*) co-localize perfectly. (*D*) Effect of the anti-βNRXN antibody on artery rings. The culture was maintained in serum-free MCDB131 medium (Sigma-Aldrich) in a humidified incubator and was stimulated for 3 days with FGF-2 10 ng/mL (R&D Systems) with 40 μg/mL of anti-βNRXN antibody or human IgG Fab$_{(2)}$. Bars indicate mean and standard deviation ($n = 5$); a representative sample of 3 experiments is shown.

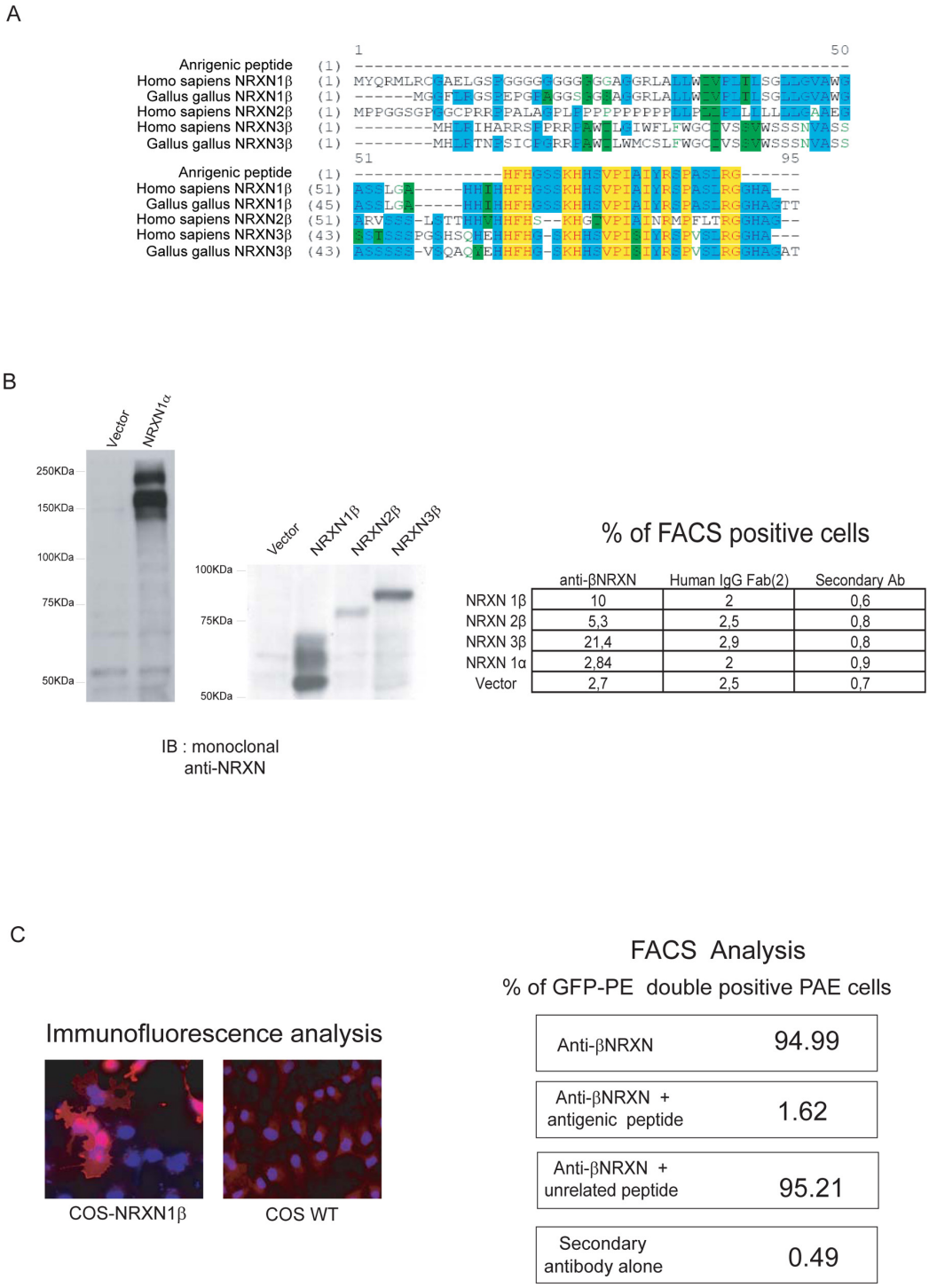

Fig. S7. Recombinant anti-βNRXN antibody characterization. (*A*) Alignment of the antigenic peptide used for the recombinant anti-βNRXN antibody selection shows high identity with *Homo sapiens* neurexins 1β and *Gallus gallus* β-neurexins. (*B*) The anti-βNRXN antibody recognizes β- but not α-neurexin by FACS analysis. HeLa cells were transiently transfected with NRXN1α- or β-neurexin 1, 2, and 3 and were blotted with the monoclonal anti-NRXN antibody to detect the amount of expressed proteins (*Left*). Although the anti-βNRXN antibody was produced against NRXN 1β, the FACS analysis (*Table*) revealed that it also can recognize the other β isoforms of neurexin. Only a background signal is detectable on the cells expressing α-neurexin or with human IgG Fab$_{(2)}$. (*C*) (*Left*) Immunofluorescence analysis performed with the anti-βNRXN antibody in COS WT cells or cells overexpressing neurexin 1β reveals the membrane localization of neurexin. The recombinant anti-βNRXN antibody stained the COS-neurexin 1β (*red*), with no specific signal in nontransfected cells. (*Right*) FACS analysis performed on a PAE neurexin 1β-GFP clone. The recombinant anti-βNRXN recognized 95% of all GFP-positive cells. The specific peptide, but not the unrelated peptide, strongly decreased the number of double-positive cells, indicating the high specificity of the anti-βNRXN antibody.

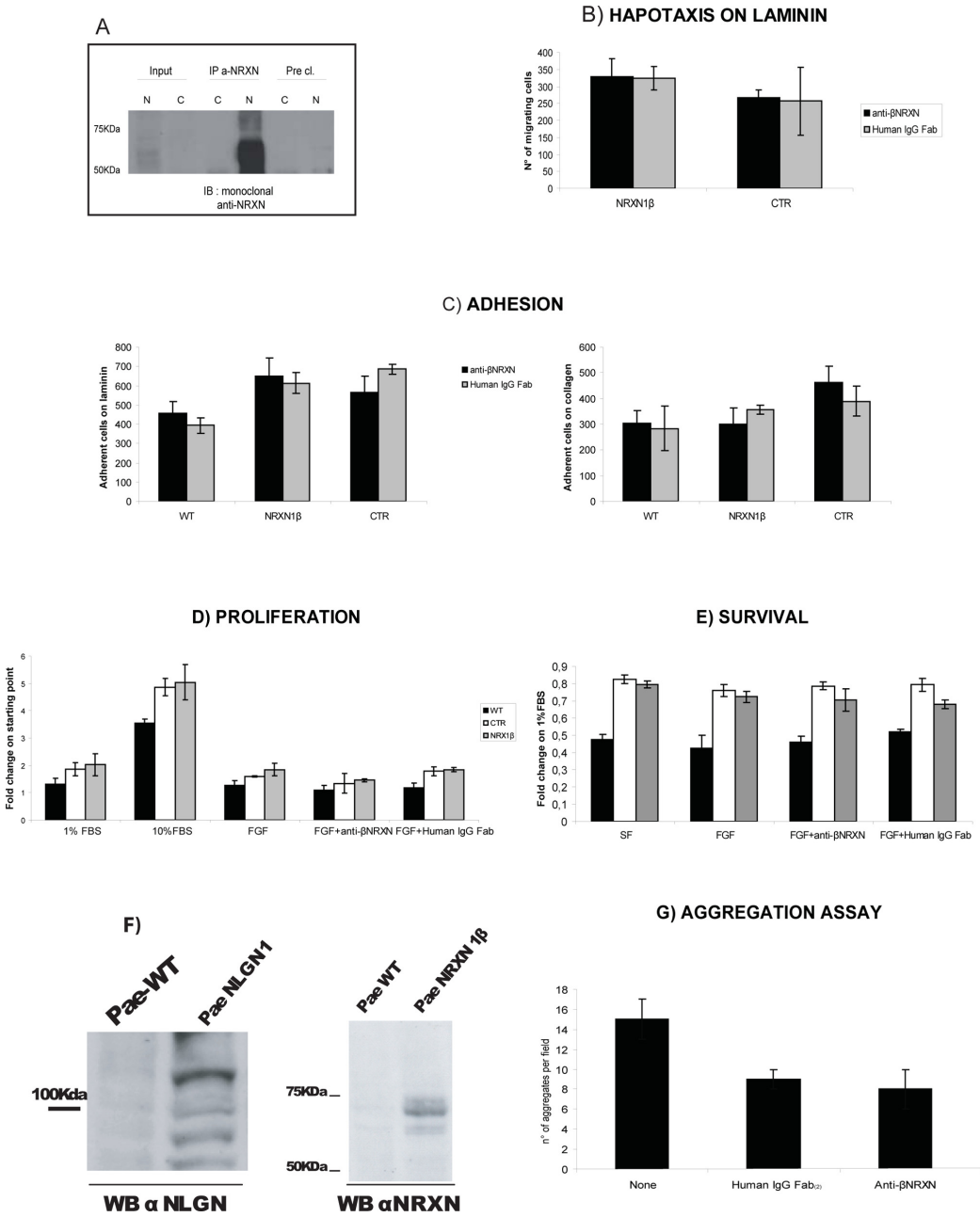

Fig. S8. Assays to detect the activity of the anti-βNRXN antibody on cell migration, adhesion, proliferation, survival, and neurexin- and neuroligin-mediated cell aggregation. (*A*) Expression of neurexin 1β in Ao cells detected by immunoprecipitation. N, neurexin 1β infection; C, control infection. (*B*) Role of anti-βNRXN antibody in migration of haptotaxis toward laminin in Ao cells. Ao cells infected with the neurexin 1β or control lentiviral vector were treated with anti-βNRXN antibody or human IgG $Fab_{(2)}$ and seeded on Transwell supports precoated with 25 μg/mL of laminin I. After 4 h migrated cells were stained with crystal violet and counted. Bars indicate the mean number of migrated cells. Error bars indicate SD. (*C*) Effect of the anti-βNRXN antibody on the adhesive properties of Ao cells overexpressing neurexin 1β on 15 μg/mL of laminin I (*Left*) or 5 μg/mL of collagen I (*Right*). Cells were treated as indicated and allowed to adhere for 30 min. Bars show the mean number of adherent cells. Error bars indicate SD. (*D*) Effect of the anti-βNRXN antibody on the proliferation activity of Ao-neurexin 1β cells. Cells were treated for 72 h as indicated and then quantified. Bars show mean fold change from starting point. Error bars show SD. (*E*) Effect of the anti-βNRXN antibody in survival of Ao-neurexin 1β cells after serum deprivation. Cells were treated for 72 h as indicated, and survival was quantified with a luminescent ATP detection assay system. Bars show mean fold change with 1% FBS treatment. Error bars show SD. (*F*) Immunoblots representing neuroligin 1 or neurexin 1β expression in PAE-neuroligin 1 or PAE-neurexin 1 clones used for the aggregation assay presented in *G*. (*G*) Role of the anti-βNRXN antibody in cell aggregation mediated by neurexin–neuroligin interaction. Pools of cells overexpressing either β-neurexin or neuroligin (*F*) were incubated in the presence of calcium ions with the anti-βNRXN antibody or human IgG $Fab_{(2)}$ and then were placed on a Burker chamber for counting. Bars represent the mean number of cell aggregates (2 or more cells counted) in at least 4 different fields. Error bars show SD.

A

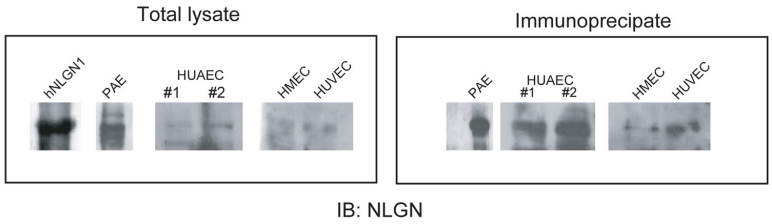

IB: NLGN

B

FIBROBLASTS

	NRXN1	NRXN2	NRXN3	NLGN1	NLGN2	NLGN3	NLGN4
DETROIT	-	-	+	+	+	+	+
DF1	-	n.t.	n.t.	+	n.t.	n.t.	+
MEF	+	-	-	+	+	+	n.t.
CEF	+	n.t.	n.t.	+	n.t.	n.t.	+
NHDF *	-	+	-	+	+	-	+

SMOOTH MUSCLE CELLS

	NRXN1	NRXN2	NRXN3	NLGN1	NLGN2	NLGN3	NLGN4
ZAC	-	-	-	+	n.t.	+	n.t.
hSMC	-	-	-	-	n.t.	n.t.	n.t.
HUASMC *	-	-	+	-	+	-	+

ENDOTHELIAL CELLS

	NRXN1	NRXN2	NRXN3	NLGN1	NLGN2	NLGN3	NLGN4
PAE	+	-	-	n.t.	+	+	n.t.
HUAEC	-	-	+	+	+	+	+
HUVEC	- *	- *	+ *	+	+	+	+
HMEC	-	-	-	-	+	+	+
Murine endothelium	n.t.	n.t.	n.t.	-	+	+	-

Neuroligin splicing pattern in EC

	Site A1	Site A2	Site B
NLGN1	-	-	+
NLGN2		+	
NLGN3	+/-	+/-	
NLGN4		+/-	

C

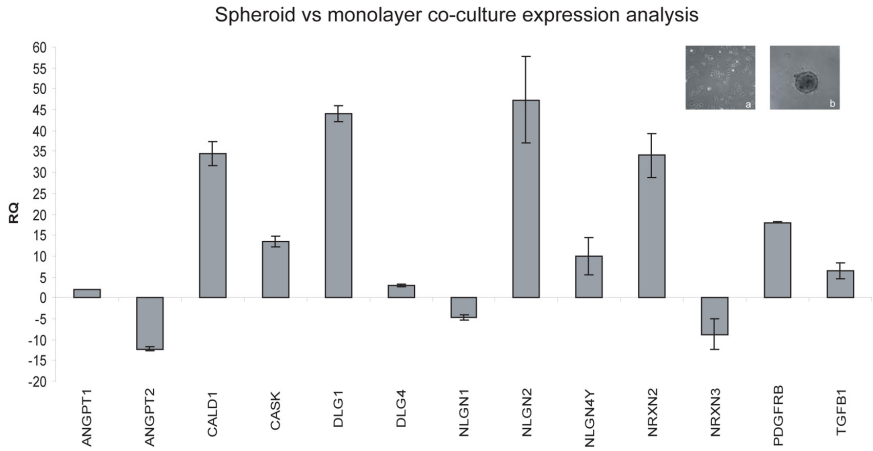

Fig. S9. Neurexin and neuroligin expression in cultured cells. (*A*) Neuroligin protein expression was detected by immunoprecipitation in ECs of different origins. A control immunoprecipitation was made with cells overexpressing human neuroligin 1. PAE, porcine aortic ECs; HUAEC, human umbilical artery ECs; HUVEC, human umbilical vein ECs; HMEC, human microvascular ECs. (*B*) Table showing results of RT-PCR analysis of neurexin and neuroligin expression in cultured ECs, VSMCs, and fibroblasts. +, isoform expressed; −, isoform not present; n.t., not tested. The expression of different neuroligin isoforms was easily detected in all cells. The table (*Right*, *Bottom Row*) shows the alternative splicing pattern for ECs. +, splice insert present; −, splice insert absent; +/−, both splicing variants detected. On the other hand, even though VSMCs express neurexin in vivo, none of the neurexin transcripts was produced consistently by in vitro-cultured VSMCs populations (*Middle*). These data corroborate the absence of detectable neurexin protein in these cells (not shown). ZAC and hVSCM mRNA was extracted at passage number 5. CEF, chicken embryo fibroblast; Detroit, human fibroblast; DF1, chicken fibroblast; hSMC, VSMCs derived from human arterioles; HUASMC, human umbilical artery smooth muscle cells; MEF, mouse embryo fibroblast; NHDF, normal human dermal fibroblast; ZAC, VSMCs derived from aortas of Zucker lean rat; *, expression data obtained by qPCR. Genes detected at >34 cycles were considered not expressed. (*C*) Analysis of transcripts levels by qPCR in a 3D co-culture of ECs and fibroblasts. The expression of neurexin and neuroligin genes is modulated along with those of some of their intracellular partners (*CASK*, *DLG1*) and blood vessel maturation markers and mediators (Cald 1, Angpt1 and 2, βPDGFR, TGFβ) in the 3D spheroid (b) compared with the monolayer co-culture (a). Results, expressed as relative quantity, are shown as mean (SEM) of 2 experiments.